Journal of Biomedical Optics

SPIEDigitalLibrary.org/jbo

Simultaneous *in vivo* imaging of melanin and lipofuscin in the retina with photoacoustic ophthalmoscopy and autofluorescence imaging

Xiangyang Zhang
Hao F. Zhang
Carmen A. Puliafito
Shuliang Jiao

SPIE

Simultaneous *in vivo* imaging of melanin and lipofuscin in the retina with photoacoustic ophthalmoscopy and autofluorescence imaging

Xiangyang Zhang,[a] Hao F. Zhang,[b] Carmen A. Puliafito,[a] and Shuliang Jiao[a]
[a]University of Southern California, Keck School of Medicine, Department of Ophthalmology, Los Angeles, California 90033
[b]Northwestern University, Department of Biomedical Engineering, Evanston, Illinois 60208

Abstract. We combined photoacoustic ophthalmoscopy (PAOM) with autofluorescence imaging for simultaneous *in vivo* imaging of dual molecular contrasts in the retina using a single light source. The dual molecular contrasts come from melanin and lipofuscin in the retinal pigment epithelium (RPE). Melanin and lipofuscin are two types of pigments and are believed to play opposite roles (protective versus exacerbate) in the RPE in the aging process. We have successfully imaged the retina of pigmented and albino rats at different ages. The experimental results showed that multimodal PAOM system can be a potentially powerful tool in the study of age-related degenerative retinal diseases. [DOI: 10.1117/1.3606569]

Keywords: ophthalmoscopy; photoacoustic image; fluorescence image; melanin; lipofuscin.

Paper 11203LR received Apr. 21, 2011; revised manuscript received Jun. 6, 2011; accepted for publication Jun. 10, 2011; published online Aug. 5, 2011.

Melanin and lipofuscin are two major pigments in the retinal pigment epithelium (RPE). RPE is a monolayer of pigmented cells located between the choriocapillaris and light-sensitive outer segments of the photoreceptors. Melanin protects RPE cells from oxidative damage by acting as an antioxidant.[1] Unfortunately, melanin may lose its protective function with aging and also can be irreversibly photobleached as a result of longtime light exposure.[2] On the other hand, lipofuscin is a by-product of phagocytosis of the photoreceptor outer segments, which accumulates with aging of the retina. Excessive levels of lipofuscin accumulation could compromise essential RPE functions and contribute to the pathogenesis of age-related macular degeneration (AMD).[3] AMD is one of the major blinding diseases affecting millions of people in the developed countries. Hence, *in vivo* imaging of melanin and lipofuscin can provide important aging information of the retina, which is important for AMD research and clinical diagnosis.[4]

To specifically image melanin and lipofuscin with optical imaging modalities, their most distinctive optical signatures should be captured. The most distinctive optical property of melanin is its high optical absorption coefficient in a wide optical spectral range. For lipofuscin, the optical signature is its fluorescent spectrum in 580 to 700 nm when excited by light of 364 to 633 nm.[5,6] The distinctive optical properties of melanin and lipofuscin can thus be sensed by photoacoustic ophthalmoscopy (PAOM)[7–10] and autofluorecence (AF) imaging when illuminated with laser pulses at 532 nm.

We have recently demonstrated the feasibility of simultaneously imaging melanin and lipofuscin in *ex vivo* ocular samples.[7] In this paper, we report on further combining PAOM with AF imaging for *in vivo* imaging of RPE melanin and lipofuscin.

Figure 1 shows a schematic of the experimental system. The illuminating light source for both PAOM and AF is a frequency-doubled Q-switched Nd:YAG laser (SPOT-10–100-532, Elforlight Ltd., UK: 532 nm; 10 μJ/pulse; 2 ns pulse duration; maximal pulse repetition rate: 30 kHz). The output laser light was first attenuated with a neutral density (ND) filter before coupled into a single mode optical fiber. The light reflected from the surface of the ND filter is detected by a photodiode (Pd1) to provide trigger signal for both AF and PAOM data acquisition. The energy of each laser pulse was also recorded by another photodiode (Pd2) to compensate for the pulse energy instability. The output laser light from the fiber was collimated into a beam diameter of 6 mm, combined with the probing light of a spectra-domain optical coherence tomography (SD-OCT) by a hot mirror (Edmund, Inc.), reflected by a dichroic mirror (DMLP567, Thorlabs, Inc.), scanned by a *X-Y* galvanometer, and finally delivered to the eye through a lens system consisting of an achromatic relay lens ($f = 60$ mm) and an objective lens ($f = 19$ mm). The configuration of the SD-OCT subsystem is similar to that reported in our previous publications,[8] which used a superluminescent diode light source with a center wavelength of 830 nm. The galvanometer scanner was controlled by an analogue-output board, whose sample clock was used to trigger the laser.

The back-traveling AF light emitted from the sample passed through the objective lens, the relay lens, the dichroic mirror, a long-pass filter (FEL0550, cut on wavelength: 550 nm, Thorlabs, Inc.), a 532 nm laser rejection filter (532-D2C, Omega Optical), and then was coupled into a multimode optical fiber (MMF) with a core diameter of 50 μm. The light exiting the MMF was detected by an avalanche photodetector (APD110A, Thorlabs, Inc.). The combination of the long-pass filter and the laser rejection filter provides an attenuation of 10^8 (OD = 8) to the reflected excitation light. The AF signal was digitized and stored by a high speed digitizer (CompuScope 22G8, Gage Applied Technologies) at a sampling rate of 2 GS/s.

The induced photoacoustic (PA) waves from the sample were detected by a custom-built needle ultrasonic transducer (30 MHz; bandwidth: 50%; active element diameter: 1 mm), which was placed in contact with the eyelid coupled by ultrasound gel. The detected PA signals were first amplified by 80 dB and then digitized by another high-speed digitizer

Address all correspondence to: Shuliang Jiao, University of Southern California, Department of Ophthalmology, 1450, San Pablo Street – DVRC 307E, Los Angeles, California 90033. Tel: 323-442-6778; Fax: 323-442-6528; E-mail: sjiao@usc.edu.

1083-3668/2011/16(8)/080504/3/$25.00

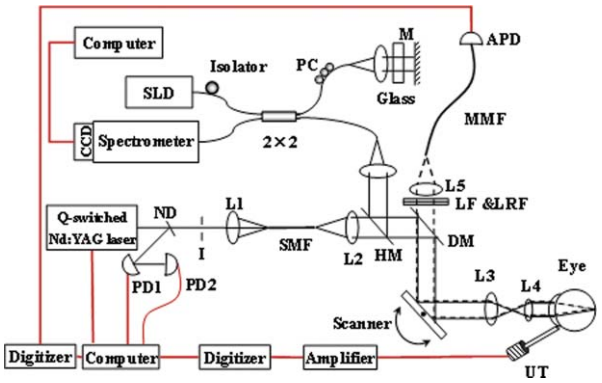

Fig. 1 Schematic of the multimodal PAOM. ND: neutral density filter. PD: photodiode; I: iris; DM: dichroic mirror; LF: longpass Filter; LRF: laser rejection filter; MMF: multimode optical fiber; APD: avalanche photodetector; UT: ultrasonic transducer; SLD: superluminescent diode; PC: polarization controller.

(CompuScope14200, Gage Applied Technologies) at a sampling rate of 200 MS/s.

As reported in our previous publications,[9] the system has a lateral resolution of 4.5 μm on the retina. The PAOM depth resolution is 23 μm, which is determined by the bandwidth and center frequency of the ultrasonic transducer. When the laser was triggered at a pulse repetition rate of 24 kHz, simultaneous acquisition of the PAOM and AF images each consisting of 256×256 pixels takes 2.7 s. The total imaging time including alignment process took about 1 to 2 min.

In our current study, the laser pulse energy was measured to be 40 nJ after the objective lens, which is lower than the ANSI safety limit. The OCT imaging system was mainly used for imaging guidance to reduce visible light exposure to the eye. During alignment, only the OCT light was on. After the retinal region of interest was identified and the OCT image was optimized, the OCT light was turned off and the PAOM imaging mode was activated.

We first measured the AF spectra of a human RPE sample and a lipofuscin control slides (American MasterTech Scientific Inc.) with a commercial spectrometer (USB4000, Ocean Optics Inc.). The similarity of the AF spectra (Fig. 2) verified the

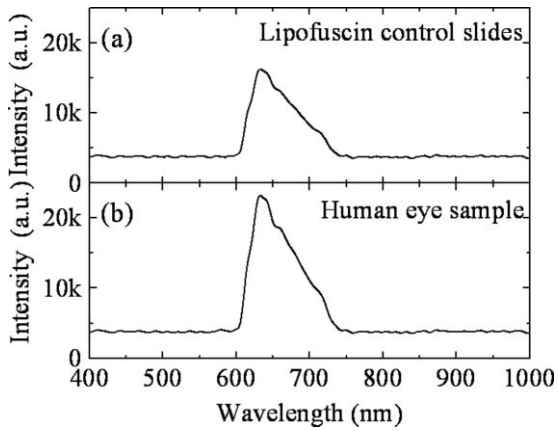

Fig. 2 (a) and (b) autofluorescent spectra of the lipofuscin and the human RPE sample with excitation wavelength of 532 nm.

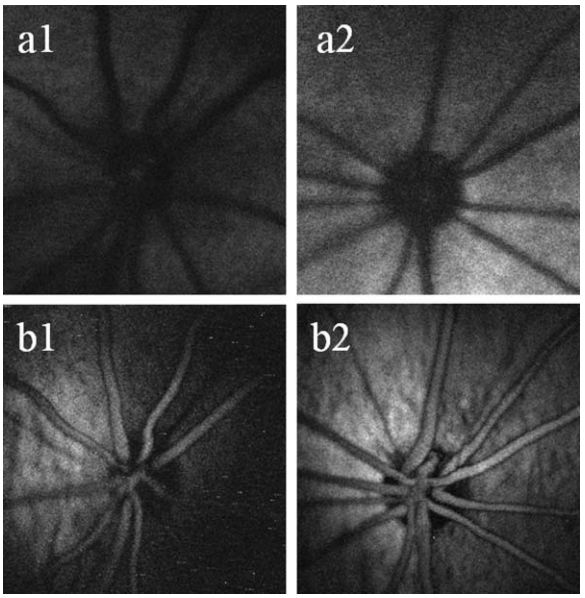

Fig. 3 AF [(a1) and (a2)] and PAOM [(b1) and (b2)] images of pigmented rats. (a1) and (b1): 10 weeks-old; (a2) and (b2): 18 weeks-old.

molecular contrast of the AF imaging. In the meantime, no PA signal was detected for the lipofuscin control slides. The results demonstrated that lipofuscin had no contribution to the PAOM image in our system. Furthermore, we have previously proved that RPE melanin has no contribution to the AF image.[7]

We imaged the eyes of long evans rats and sprague dawley rats (body weight: 200 to 700 g, Charles Rivers) with normal retina to assess the imaging capability for pigmented and albino rats. For each breed, two rats of 10 weeks old and two rats of 18 weeks old were imaged. The animals were anesthetized by intraperitoneal (IP) injection of a cocktail containing Ketamine (90 mg/kg body weight) and Xylazine (10 mg/kg body weight). In the meantime, the pupils were dilated with 10% Phenylephrine solution. After anesthetization, the animals were restrained in a mounting tube, which was fixed on a five-axis platform. Raster scans with the fast axis along the horizontal direction were performed. The scan angle was approximately 20 deg for imaging the rat retina. All experiments were performed in compliance with the guidelines of the University of Southern California's Institutional Animal Care and Use Committee.

Figures 3(a1) and 3(a2) shows the AF images of the retina of pigmented rats at 10 weeks old and 18 weeks old, respectively. Figures 3(b1) and 3(b2) show PAOM images of the retina of pigmented rats at 10 weeks old and 18 weeks old, respectively. Figure 4 shows the AF and PAOM images of the albino rats with the same ages as in Fig. 3. The images demonstrated that the AF and PAOM imaging modes are perfectly registered. The AF retinal images represent the lipofuscin distribution in the RPE: the stronger the AF signals the higher the lipofuscin concentration. In both the pigmented and albino rats we can see that lipofuscin concentration increased with age, which is in agreement with the literature.[10] From the images we can also see that for the same age the intensity of autofluorescence from the albino rat RPE is higher than that from the pigmented rat RPE. There are significant differences in the appearance of the

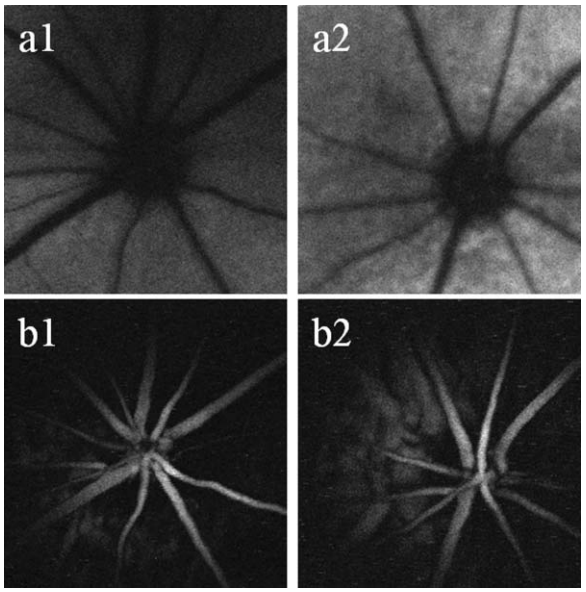

Fig. 4 AF [(a1) and (a2)] and PAOM [(b1) and (b2)] images of albino rats. (a1) and (b1): 10 weeks-old; (a2) and (b2): 18 weeks-old.

PAOM images between the pigmented and albino rats. Since there is no melanin in the RPE of the albino rats, the RPE layer did not show up in the PAOM images. Instead, the laser light penetrated the RPE and generated PA signals in the choroidal blood vessels. In contrast, in the pigmented rats the RPE layer appears as the brightest layer in the PAOM images. Due to the fact that the laser light was totally blocked by the RPE layer, no signal from the choroidal vessels can be observed.

To further demonstrate the accumulation of lipofuscin with age, we calculated the histogram of AF intensity in Fig. 3 and Fig. 4. The results are shown in Fig. 5. From the histogram, we can clearly see that the distribution of the AF intensity increased significantly with aging. For the same age, the AF intensity of albino rats is stronger than that of a pigmented rat. When the rats become older, the increase of the AF intensity is obvious, especially in the albino rats. The experiments showed evidence of increased lipofuscin concentration with aging. Possibly due to the protective functions of RPE melanin in the pigmented rats, the increase of lipofuscin concentration is not as significant as in the albino rats.

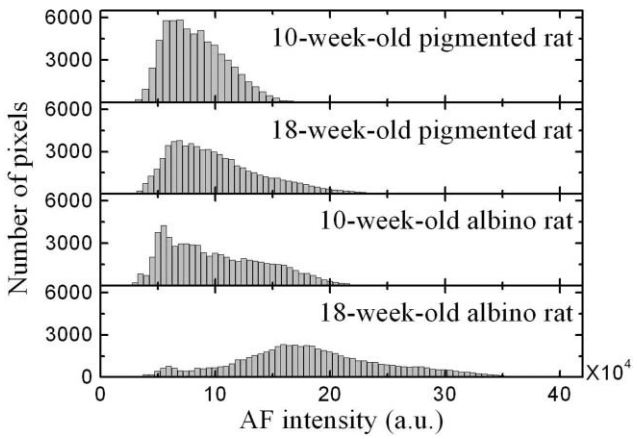

Fig. 5 Calculated AF intensity distributions of the different rats.

In conclusion, we have achieved simultaneous *in vivo* imaging of the RPE melanin and lipofuscin in rat eyes with multimodal PAOM. The experiments here just represent a preliminary test of the capability of the imaging system. For the next step, we need to extract quantitative lipofuscin and melanin distribution from the multimodal PAOM images. We are exploring a new metric for grading the aging status of the RPE cells by using PAOM.

Acknowledgments

This work is supported in part by the following grants: National Institutes of Health Grant No. 7R21EB008800-02 (Jiao), Coulter Translational Award (Jiao), and National Institutes of Health Grant No. 1RC4EY021357 (Zhang).

References

1. M. A. Ostrovsky, N. L. Sakina, and A. E. Dontsov, "An antioxidative role of ocular screening pigments," *Vision Res.* **27**(6), 893–899 (1987).
2. T. Sarna, J. M. Burke, W. Korytowski, M. Rozanowska, C. M. B. Skumatz, A. Zareba, and M. Zareba, "Loss of melanin from human RPE with aging: possible role of melanin photooxidation," *Exp. Eye Res.* **76**(1), 89–98 (2003).
3. F. C. Delori, D. G. Goger, and C. K. Dorey, "Age-related accumulation and spatial distribution of lipofuscin in RPE of normal subjects," *Invest. Ophthalmol. Vis. Sci.* **42**(8), 1855–1866 (2001).
4. J. J. Weiter, F. C. Delori, G. L. Wing, and K. A. Fitch, "Retinal pigment epithelial lipofuscin and melanin and choroidal melanin in human eyes," *Invest. Ophthalmol. Vis. Sci.* **27**(2), 145–152 (1986).
5. A. D. Marmorstein, L. Y. Marmorstein, H. Sakaguchi, and J. G. Hollyfield, "Spectral profiling of autofluorescence associated with lipofuscin, Bruch's membrane, and sub-RPE deposits in normal and AMD eyes," *Invest. Ophthalmol. Vis. Sci.* **43**(7), 2435–2441 (2002).
6. F. C. Delori, C. K. Dorey, G. Staurenghi, O. Arend, D. G. Goger, and J. J. Weiter, "*In vivo* fluorescence of the ocular fundus exhibits retinal pigment epithelium lipofuscin characteristics," *Invest. Ophthalmol. Vis. Sci.* **36**(3), 718–729 (1995).
7. X. Zhang, M. Jiang, A. A. Fawzi, X. Li, K. K. Shung, C. A. Puliafito, H. F. Zhang, and S. Jiao, "Simultaneous dual molecular contrasts provided by the absorbed photons in photoacoustic microscopy," *Opt. Lett.* **35**(23), 4018–4020 (2010).
8. S. Jiao, M. Jiang, J. Hu, A. Fawzi, Q. Zhou, K. K. Shung, C. A. Puliafito, and H. F. Zhang, "Photoacoustic ophthalmoscopy for *in vivo* retinal imaging," *Opt. Express* **18**(4), 3967–3972 (2010).
9. S. Jiao, Z. Xie, H. F. Zhang, and C. A. Puliafito, "Simultaneous multimodal imaging with integrated photoacoustic microscopy and optical coherence tomography," *Opt. Lett.* **34**(19), 2961–2963 (2009).
10. P. Mukherjee, S. Bose, A. A. Hurd, R. Adhikary, H. Schonenbrucher, A. N. Hamir, J. A. Richt, T. A. Casey, M. A. Rasmussen, and J. W. Petrich, "Monitoring the accumulation of lipofuscin in aging murine eyes by fluorescence spectroscopy," *Photochem. Photobiol.* **85**, 234–238 (2009).